Infrared phonon spectroscopy of a compressively strained (001) $SrTiO_3$ film grown on a (110) $NdGaO_3$ substrate

2011 J. Phys.: Condens. Matter 23 045901

(http://iopscience.iop.org/0953-8984/23/4/045901)

IOP Publishing — Journal of Physics: Condensed Matter
J. Phys.: Condens. Matter **23** (2011) 045901 (8pp) doi:10.1088/0953-8984/23/4/045901

Infrared phonon spectroscopy of a compressively strained (001) $SrTiO_3$ film grown on a (110) $NdGaO_3$ substrate

D Nuzhnyy[1], J Petzelt[1], S Kamba[1], X Martí[2], T Čechal[2], C M Brooks[3,4] and D G Schlom[3]

[1] Institute of Physics, Academy of Sciences of the Czech Republic, Na Slovance 2, 18221 Praha 8, Czech Republic
[2] Department of Condensed Matter Physics, Charles University, 12116 Prague, Czech Republic
[3] Department of Materials Science and Engineering, Cornell University, Ithaca, NY 14853-1501, USA
[4] Department of Materials Science and Engineering, Penn State University, University Park, PA 16802-5005, USA

Received 15 November 2010
Published 7 January 2011
Online at stacks.iop.org/JPhysCM/23/045901

Abstract
Polarized infrared reflectivity was measured between 5 and 300 K on a 17 nm thick, 1.1% compressively strained epitaxial (001) $SrTiO_3$ film and the orthorhombic (110) $NdGaO_3$ substrate upon which it was grown. A strong in-plane infrared anisotropy of the $NdGaO_3$ substrate was observed and polar modes with B_{1u}-and a mixture of $B_{2u} + B_{3u}$-symmetry were seen. At low temperatures three new modes arose in the 90–130 cm^{-1} range, which we assigned to 4f Nd electronic transitions. The in-plane $SrTiO_3$ film phonons showed strong stiffening compared to the phonon frequencies of bulk unstrained $SrTiO_3$, particularly the soft mode, and the in-plane phonon peaks were found to split. No anomalies were detected as a function of temperature in either the infrared response or lattice parameters of the compressively strained $SrTiO_3$ film, providing an absence of evidence for the out-of-plane ferroelectric phase transition predicted by theory.

(Some figures in this article are in colour only in the electronic version)

1. Introduction

After more than two decades of intense research it has become clear that dielectric properties, as well as many other properties of ferroelectric and related materials, differ significantly from bulk intrinsic properties when in thin film form [1–6]. This occurs for both polycrystalline and epitaxial films. In high-quality epitaxial films the dominant effect is from stress in the film caused by the lattice mismatch between the film and substrate or, in the case where this misfit strain is larger, by the difference in thermal expansion of the film and substrate. The theories based on the Landau–Ginzburg approach to ferroelectric phase transitions, first-principles calculations, and experiments show that the dielectric properties in high-permittivity materials are extremely sensitive to such strains. For instance, the ~1% in-plane tensile strain in a $SrTiO_3$ film on a $DyScO_3$ substrate induces a ferroelectric phase transition near room temperature [7] in coexistence with the antiferrodistortive phase below ~180 K, while no ferroelectric phase exists in the unstrained bulk incipient ferroelectric $SrTiO_3$ [8, 9]. The strain-induced spontaneous polarization $\boldsymbol{P}_s$ lies in the film plane in the former case.

Many device applications in nanoelectronics require polarization switching involving an out-of-plane polarization, $\boldsymbol{P}_s$. Theories [4–7, 10–13] predict that this could be induced in $SrTiO_3$ films by a compressive in-plane stress. Studies have been performed on compressively strained $SrTiO_3$ epitaxial films on several substrates, including (110) $NdGaO_3$, (001) $(LaAlO_3)_{0.29}$–$(SrAl_{1/2}Ta_{1/2}O_3)_{0.71}$ (LSAT), and silicon. Films on $NdGaO_3$ displayed evidence of a ferroelectric phase transition near 150 K using infrared (IR) spectroscopy [14]. $SrTiO_3$ on LSAT was studied by SHG and dielectric measurements [15, 16], but no evidence of a ferroelectric phase transition was found [17, 18]. Recently, $SrTiO_3$ films grown directly on (001) Si by molecular-beam epitaxy (MBE) were shown to be ferroelectric up to room temperature [19]. Due to the large compressive strain of ~1.7%, only films of thickness below ~3 nm were shown to be commensurate and ferroelectric up to room temperature. The ~8 nm thick $SrTiO_3$/Si film was relaxed and did not display ferroelectricity [19]. Two recent papers [16, 20] reported out-of-plane ferroelectricity up to room temperature in thicker $SrTiO_3$ films of thicknesses ~60 and ~100 nm, respectively. The 100 nm thick film was grown on a single-crystal $SrTiO_3$ substrate by pulsed-laser deposition (PLD) in reduced oxygen atmosphere. Its remnant polarization P_r, which survived from low temperatures up to 300 K, was of the order of several $\mu C\ cm^{-2}$ and increased with increasing oxygen deficiency. It has been suggested [21] that the origin of the ferroelectricity in such homoepitaxial films is due to correlated defect complexes, in this case a Sr vacancy adjacent to an oxygen vacancy producing a SrO vacancy. The 60 nm thick $SrTiO_3/NdGaO_3$ film grown by PLD showed a very smeared P_r, which increases steeply to several $\mu C\ cm^{-2}$ only below ~100 K and shows a very narrow hysteresis loop. These features together with the typical dielectric dispersion below ~150 K were assigned to relaxor ferroelectric behavior [16]. Very recently [22], long-range ferroelectric order below ~700 K with an out-of-plane $\boldsymbol{P}_s$ has been observed also in a compressively strained (2.1%) 9 nm thick $KTaO_3$ film grown by PLD on a conductive $SrTiO_3$ substrate. Bulk $KTaO_3$ is another classic incipient ferroelectric without a ferroelectric transition down to 0 K.

In this paper we report on a study of an epitaxial (001) $SrTiO_3$ film grown by MBE on a (110) $NdGaO_3$ substrate, using a novel IR reflectance technique to study the temperature behavior of the in-plane polar phonons, including the soft mode [9, 14, 17]. The reason for this study is because of the strong anisotropy in the IR range due to structure of the (110) $NdGaO_3$ substrate, which had not been fully characterized in previous IR reports on $NdGaO_3$ single crystals [23–25] and was neglected in the previous $SrTiO_3/NdGaO_3$ film study [14].

In the past, IR and THz transmission spectroscopy was successfully used for characterizing the polar phonons in ferroelectric thin-films, particularly for the soft mode studies in $SrTiO_3$ films [26–31]. The IR reflection technique, which has been more used recently [9, 14, 17], has some advantages over the transmission measurement mode in that it characterizes a broader spectral range, since in most cases it can be used in a broad spectral range where the substrate is opaque. It enables the characterization of all polar phonon modes, and the sensitivity is in many cases enhanced compared to transmission due to an effectively thicker optical path of the multiple reflected beams from both surfaces of the film. It must be noted, however, that the sensitivity depends in a nontrivial way on the optical parameters of the substrate, whose dielectric spectrum varies quite strongly in the reststrahl region. We have also revealed that metallic substrates with a negative permittivity in the IR range strongly diminish the accuracy of determining the phonon parameters of the film. Therefore dielectric substrates without electrodes are preferred for this technique.

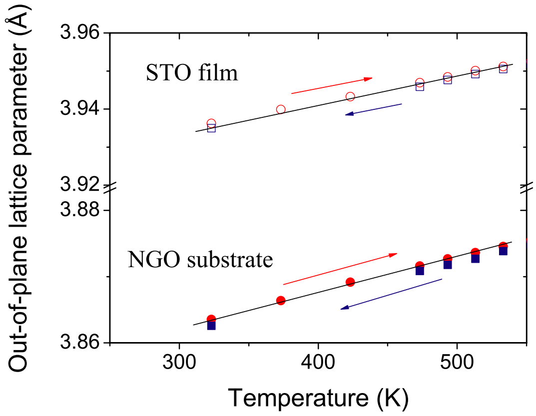

Figure 1. Out-of-plane lattice parameters of the (001) $SrTiO_3$ film and the underlying (110) $NdGaO_3$ substrate upon which it was grown as a function of temperature on heating (circles) and cooling (squares).

2. Experiment and data evaluation

The $SrTiO_3$ film was grown on a (110) $NdGaO_3$ single-crystal substrate in a Veeco 930 oxide MBE system at a substrate temperature of 650 °C in a background pressure of 5×10^{-7} Torr of O_2 with 10% O_3. The details of the growth process are outlined elsewhere [32].

The deposited (001) $SrTiO_3$ film was characterized by x-ray diffraction. The out-of-plane lattice parameter was investigated as a function of temperature using Cu Kα radiation in a PANalytical two-circle diffractometer with a parabolic mirror on the incident beam path. The sample was mounted inside an evacuated chamber and heated up to 770 K by a radiant heater while diffraction was measured using a position-sensitive detector. Room-temperature in-plane lattice parameters were investigated using a four-circle diffractometer. Data indicate that the $SrTiO_3$ film is commensurately strained to the (110) $NdGaO_3$ substrate with in-plane lattice parameters $a = b = 3.863(5)$ Å and out-of-plane lattice spacing $c = 3.941(5)$ Å. The compressive in-plane strain was +1.1%.

Second-harmonic generation measurement of another $SrTiO_3/NdGaO_3$ film [15] revealed a signal below 400 K indicating symmetry breaking and the formation of the ferroelectric phase. In a compressively strained film the spontaneous polarization should arise perpendicularly to the film plane and some anomalous temperature dependence of the c lattice parameter could be expected [4]. Figure 1 shows the temperature dependence of the obtained out-of-plane lattice parameters of the (110) $NdGaO_3$ substrate and the (001) $SrTiO_3$ film. Circles denote measurements done while heating up the sample, squares correspond to cooling down. The data show no anomalies in the explored temperature region so that our data give no support to any sharp phase transition above 300 K. This is in agreement with the aforementioned recent findings on PLD-grown $SrTiO_3/NdGaO_3$ films [16].

The IR reflectance measurements under near-normal incidence of the polarized light were performed using a FTIR Bruker IFS 113v spectrometer equipped with a He-cooled (1.5 K) Si bolometer over the 5–300 K temperature range. The bare $NdGaO_3$ substrate and 17 nm thick $SrTiO_3$ film deposited on the same substrate were measured in two polarizations ($\boldsymbol{E} \parallel [001]$ and $\boldsymbol{E} \parallel [110]$ with respect to the (110) $NdGaO_3$ substrate) at the same conditions on cooling down to 5 K in an Optistat CF cryostat (Oxford Instruments). The thick polyethylene windows used permit IR measurements only up to 650 cm^{-1}.

The dielectric response of the bare substrate was evaluated from fitting the IR reflectivity spectra

$$R(\omega) = \left| \frac{\sqrt{\varepsilon^*(\omega)} - 1}{\sqrt{\varepsilon^*(\omega)} + 1} \right|^2 \tag{1}$$

with the factorized form of the complex permittivity [33]

$$\varepsilon^*(\omega) = \varepsilon_\infty \prod_j \frac{\omega_{\mathrm{LO}j}^2 - \omega^2 + \mathrm{i}\omega\gamma_{\mathrm{LO}j}}{\omega_{\mathrm{TO}j}^2 - \omega^2 + \mathrm{i}\omega\gamma_{\mathrm{TO}j}}. \tag{2}$$

$\omega_{\mathrm{TO}j}$ and $\omega_{\mathrm{LO}j}$ are the frequencies of the jth transverse optic (TO) and longitudinal optic (LO) polar mode, respectively, $\gamma_{\mathrm{TO}j}$ and $\gamma_{\mathrm{LO}j}$ are their damping constants and ε_∞ is high-frequency (electronic) contribution to the permittivity.

The obtained fixed parameters were used for fitting the IR reflectance spectra of the $SrTiO_3/NdGaO_3$ sample as a two-slab system, by assuming the dielectric function of the $SrTiO_3$ film to have the form of a sum of n independent damped harmonic oscillators

$$\varepsilon^*(\omega) = \varepsilon_\infty + \sum_{j=1}^{n} \frac{\Delta\varepsilon_j \omega_{\mathrm{TO}j}^2}{\omega_{\mathrm{TO}j}^2 - \omega^2 + \mathrm{i}\omega\gamma_{\mathrm{TO}j}} \tag{3}$$

representing the in-plane TO phonon modes of the film, where $\Delta\varepsilon_j$ is the dielectric strength of the jth mode.

3. Results and discussion

3.1. IR spectroscopy of the (110) $NdGaO_3$ substrate

The previously reported IR reflectivity [23, 24] and THz transmission data [25] on $NdGaO_3$ single crystals have been obtained in unpolarized light, neglecting the in-plane anisotropy of the orthorhombic slab. We have revealed that the IR anisotropy of such a (110) plate is quite pronounced and influences the evaluation of the film phonon parameters on such a substrate. Because of this anisotropy we first measured the temperature dependent IR reflectivity of the bare (110) $NdGaO_3$ substrate in polarized light, which allowed us to determine the $\boldsymbol{E} \parallel \boldsymbol{c}$ and $\boldsymbol{E} \parallel [110]$ response (in the orthorhombic axes notation), since the wavevector $\boldsymbol{k}$ of our probing (transverse) IR wave is almost normal to the sample slab. Factor-group analysis for the $NdGaO_3$ with the space group *Pbnm* (number of formula units in the unit cell $Z = 4$) yields for the Brillouin-zone center (Γ-point) the following phonon modes [34]:

$$7\mathrm{A}_1\mathrm{g}(aa, bb, cc) + 5\mathrm{B}_{1\mathrm{g}}(ab) + 7\mathrm{B}_{2\mathrm{g}}(ac) + 5\mathrm{B}_{3\mathrm{g}}(bc) + 8\mathrm{A}_{1\mathrm{u}}(-) + 10\mathrm{B}_{1\mathrm{u}}(c) + 8\mathrm{B}_{2\mathrm{u}}(b) + 10\mathrm{B}_{3\mathrm{u}}(a).$$

Three of these modes, $1\mathrm{B}_{1\mathrm{u}} + 1\mathrm{B}_{2\mathrm{u}} + 1\mathrm{B}_{3\mathrm{u}}$ are acoustic modes and the remaining modes are optic. In the parentheses the

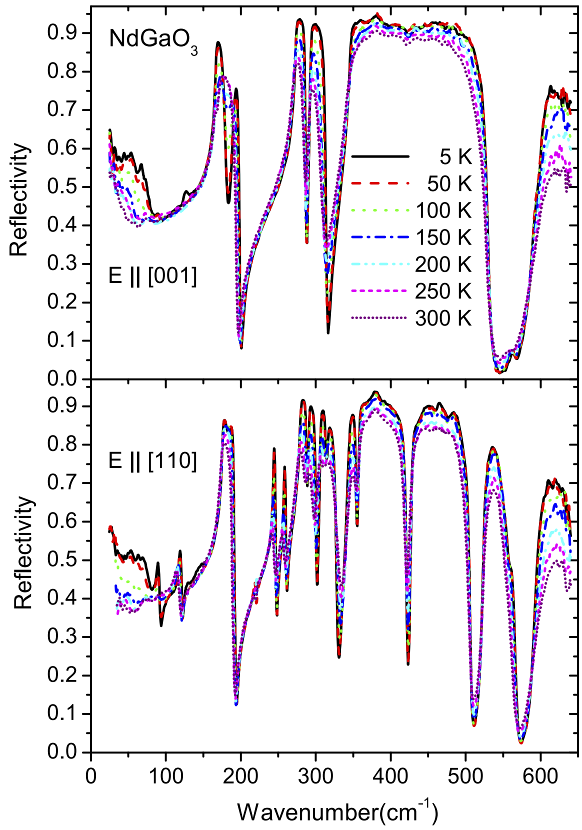

Figure 2. Polarized IR reflectivity spectra of a bare (110) $NdGaO_3$ substrate at selected temperatures.

Raman and IR activities are denoted, a, b, and c, describe the direction of the electric dipole moment of the IR-active mode and ij ($i, j = a, b, c$) denotes the Raman activity (direction of $\boldsymbol{E}$ in the incident and scattered wave, respectively). Therefore the IR selection rules predict $9B_{1\mathrm{u}}$ modes for $\boldsymbol{E} \parallel c$ and the mixture of $7\mathrm{B}_{2\mathrm{u}}$ and $9\mathrm{B}_{3\mathrm{u}}$ modes for the $\boldsymbol{E} \parallel [110]$ polarization with half of their oscillator strengths compared to the IR response in the principal $\boldsymbol{E} \parallel b$ and $\boldsymbol{E} \parallel a$ directions, respectively. The $\mathrm{A}_{1\mathrm{u}}$ modes are optically inactive (silent). The selection rules should be independent of temperature from $\sim$10 up to $\sim$1200 K because the space group of $NdGaO_3$ does not change [35, 36] even if some weak dielectric anomalies near $\sim$240 K and weak magnetic anomalies near $\sim$190 K (without long-range magnetic ordering) were observed [37].

In figure 2 we present the polarized IR reflectivity spectra for selected temperatures at 5–300 K in the 30–650 cm^{-1} spectral range. In the low-frequency range below $\sim$100 cm^{-1} the sample becomes partially translucent at low temperatures so that the increase of the reflectivity at the low-frequency end is due to multiple reflections from both sample surfaces. This part was not considered for the fitting, which assumes reflection from a semi-infinite surface.

In figure 3 we plot the calculated complex dielectric functions $\varepsilon_c(\omega)$ at several temperatures from the fits of the $\boldsymbol{E} \parallel c$ reflectivity spectra, which represent the response function of the $\mathrm{B}_{1\mathrm{u}}$ modes. It is clearly seen that at low temperatures all the predicted modes are revealed, but with

Table 1. Parameters of the B_{1u} polar modes in $NdGaO_3$ obtained from the fit of polarized $\boldsymbol{E} \parallel [001]$ IR reflectivity at 300 and 5 K. Frequencies ω_{TOj} and ω_{LOj} and dampings γ_{TOj} and γ_{LOj} of modes are in cm^{-1}, $\Delta\varepsilon_j$ is the dielectric strength and $\varepsilon_\infty = 3.93$.

	300 K					5 K				
No.	ω_{TOj}	γ_{TOj}	ω_{LOj}	γ_{LOj}	$\Delta\varepsilon_j$	ω_{TOj}	γ_{TOj}	ω_{LOj}	γ_{LOj}	$\Delta\varepsilon_j$
1						130.9	11.8	131.9	12.3	0.4
2	166.6	5.2	167.5	4.4	1.5	167.2	2.5	168.5	4.6	3.9
3	170.3	7.5	181.3	21.1	3.8	168.8	4.6	180.9	8.2	0.8
4	182.9	17.9	194.4	5.2	0.3	189.5	6.2	198.9	1.9	0.9
5	270.8	7.2	285.0	6.5	3.9	272.9	3.1	286.5	1.5	4.4
6	291.4	7.0	308.8	13.6	1.0	291.6	2.3	314.6	3.6	1.1
7	341.7	17.3	421.1	84.9	3.5	344.3	6.9	422.5	57.7	3.1
8	426.1	86.3	529.5	19.3	0.2	425.6	58.6	530.2	5.3	0.1
9	554.5	17.7	556.7	17.3	0.01	560.5	13.5	564.3	14.2	0.03
10	588.5	35.4	652.0	11.6	0.2	591.6	10.1	652.0	9.7	0.22

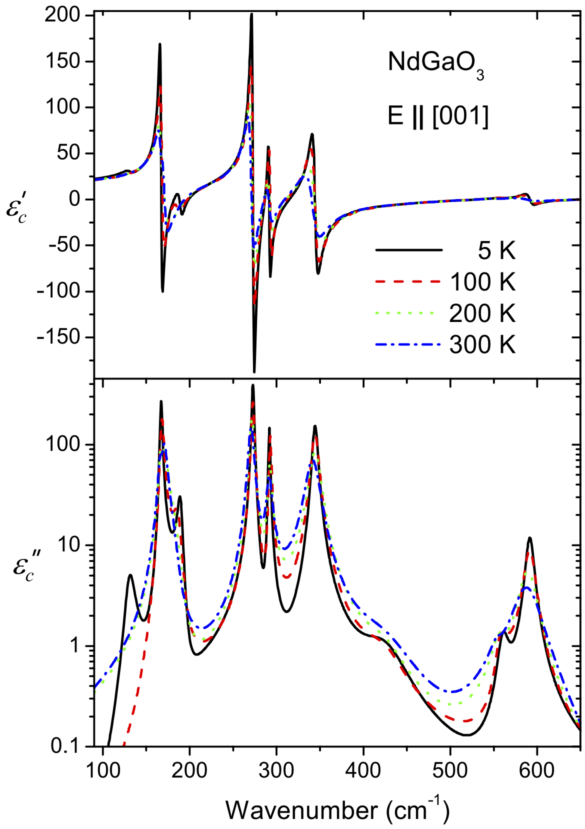

Figure 3. Real and imaginary part of the $\varepsilon_c^*(\omega)$ dielectric function of the (110) $NdGaO_3$ substrate obtained from fitting its $\boldsymbol{E} \parallel [001]$ polarized IR reflectivity spectra.

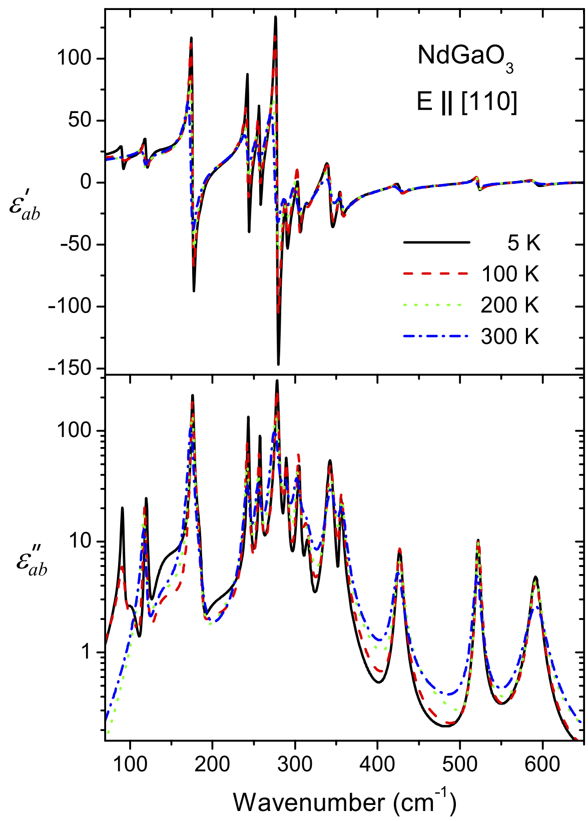

Figure 4. Real and imaginary parts of the dielectric function of the (110) $NdGaO_3$ substrate obtained from fitting the $\boldsymbol{E} \parallel [110]$ polarized IR spectra. The function represents an arithmetic mean of the $\varepsilon_a^*(\omega)$ and $\varepsilon_b^*(\omega)$ functions.

increasing temperature the mode at 131 cm^{-1} effectively vanishes. It appears that this mode could be of electronic origin (crystal field splitting of the $4f^3$ Nd levels of the $^4I_{9/2}$ multiplet), as observed in Raman scattering and deduced from optical absorption [38, 39]. Parameters of the fit at 5 and 300 K are shown in table 1 along with the calculated dielectric strengths of the polar phonons (their contributions to static permittivity) [33]

$$\Delta\varepsilon_j = \frac{\varepsilon_\infty}{\omega_{TOj}^2} \frac{\prod_k (\omega_{LOk}^2 - \omega_{TOj}^2)}{\prod_{k \neq j} (\omega_{TOk}^2 - \omega_{TOj}^2)}. \quad (4)$$

In figure 4 we plot the calculated dielectric function $\varepsilon_{ab}(\omega)$ in the $\boldsymbol{E} \parallel [110]$ direction while the fit parameters are listed in table 2. Again a low-frequency doublet (at 91 and 109 cm^{-1}) out of the 17 fitted modes vanishes on heating, which can also be assigned to the 4f Nd electronic transitions. The remaining 15 modes are in a good agreement with the $16(B_{2u} + B_{3u})$ predicted modes. As also appears from the tables 1 and 2, only modes below 200 cm^{-1} are appreciably temperature dependent. We have plotted their temperature dependent TO frequencies in figure 5.

Table 2. Parameters of the ($B_{2u} + B_{3u}$) polar modes in $NdGaO_3$ obtained from the fit of polarized $\boldsymbol{E} \parallel [110]$ IR reflectivity at 300 and 5 K. Frequencies ω_{TOj} and ω_{LOj} and dampings γ_{TOj} and γ_{LOj} of modes are in cm^{-1}, $\Delta\varepsilon_j$ is the dielectric strength and $\varepsilon_\infty = 3.2$.

	300 K					5 K				
No.	ω_{TOj}	γ_{TOj}	ω_{LOj}	γ_{LOj}	$\Delta\varepsilon_j$	ω_{TOj}	γ_{TOj}	ω_{LOj}	γ_{LOj}	$\Delta\varepsilon_j$
1						91.1	3.0	92.2	2.5	0.6
2						109.0	33.3	109.1	25.2	0.1
3	117.4	5.6	118.7	4.5	0.6	119.7	3.3	121.3	3.1	1.1
4	131.1	53.2	134.2	58.4	1.0	130.8	52.8	141.5	73.9	3.2
5	173.7	6.0	184.4	14.4	3.3	175.9	2.9	183.8	10.6	2.5
6	185.2	13.2	190.3	4.0	0.1	185.3	8.0	192.9	2.8	0.2
7	242.0	7.0	244.9	6.6	0.8	243.4	2.0	247.4	2.5	1.0
8	255.1	6.7	257.8	6.7	0.7	257.5	2.1	260.4	2.8	0.6
9	275.2	9.3	284.9	8.5	3.3	278.4	3.3	287.4	3.1	3.3
10	287.9	9.1	296.5	9.2	0.7	289.5	3.6	300.9	4.5	0.6
11	302.0	9.1	309.7	12.3	0.9	305	3.9	313.4	7.1	0.6
12	312.0	14.4	330.9	12.8	0.4	315.2	8.0	329.0	5.6	0.2
13	343.2	12.9	353.7	9.1	1.0	342.6	7.6	353.8	2.4	1.2
14	356.6	9.4	419.4	12.2	0.4	355.3	3.8	421.2	6.9	0.2
15	424.5	12.6	506.4	10.4	0.1	426.7	7.2	505.8	5.5	0.1
16	520.4	8.8	560.5	19.0	0.1	521.7	4.6	562.3	12.8	0.1
17	591.6	24.3	646.0	22.6	0.1	591.6	12.4	646.5	13.7	0.1

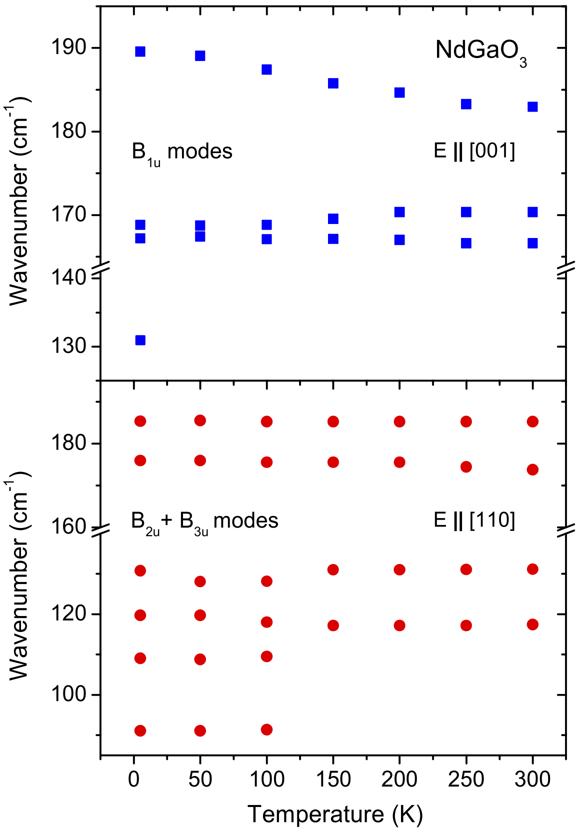

Figure 5. Temperature dependence of the low-frequency polar mode frequencies of the (110) $NdGaO_3$ substrate obtained from fitting the polarized IR reflectivity spectra. $\boldsymbol{E} \parallel [001]$ polarization yields the B_{1u}-symmetry modes and $\boldsymbol{E} \parallel [110]$ polarization yields the $B_{2u} + B_{3u}$-symmetry modes.

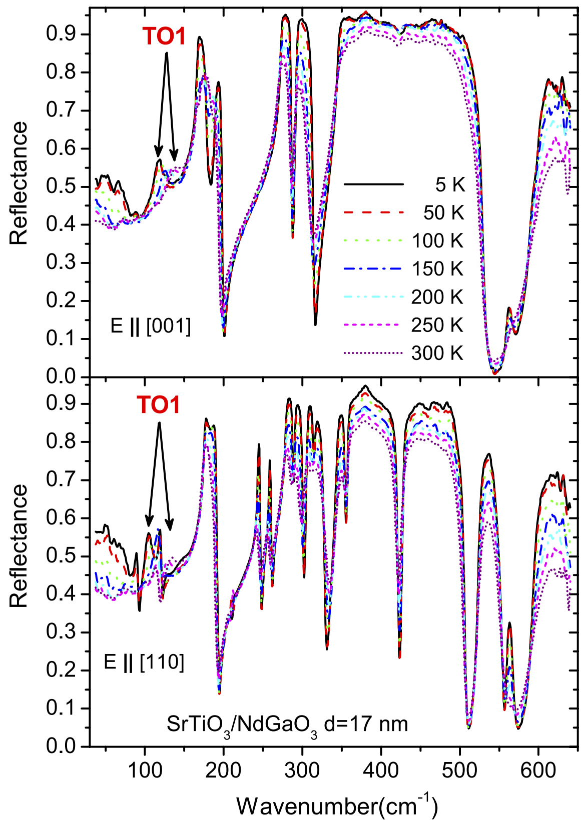

Figure 6. Polarized IR reflectance of the 17 nm (001) $SrTiO_3$ film on the (110) $NdGaO_3$ substrate.

3.2. IR spectroscopy of the $SrTiO_3$ film

In figure 6 we plot the polarized reflectance of our $SrTiO_3/NdGaO_3$ sample, which differs from the bare substrate reflectivity in several spectral regions, mainly below ~150 and near 560 cm^{-1}. The spectral fit of the two-layer system using the known bare $NdGaO_3$ substrate fit parameters enables us to obtain both the $\varepsilon_c(\omega)$ and $\varepsilon_{ab}(\omega)$ dielectric functions of the $SrTiO_3$ film, as shown in figures 7 and 8 respectively. This is shown only below 200 cm^{-1} as the high-frequency TO4 mode doublet at 561 + 563 cm^{-1} does not show any appreciable

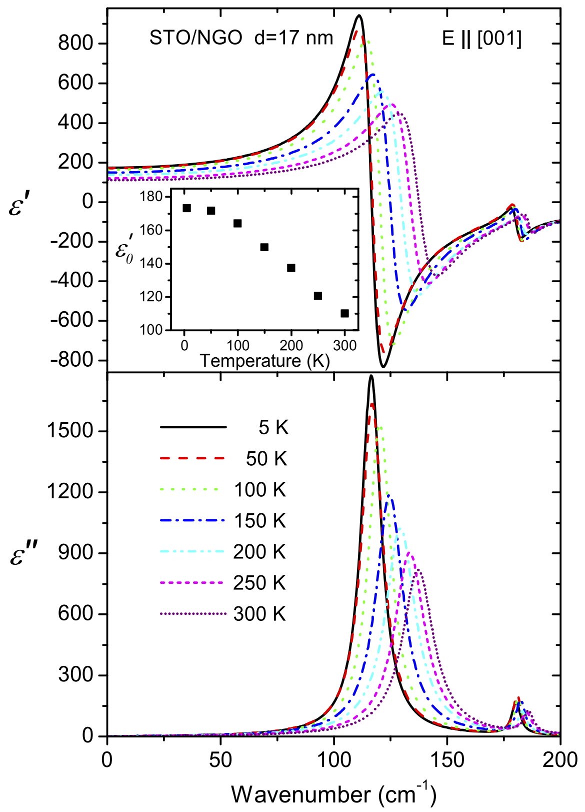

Figure 7. Complex dielectric function of the $SrTiO_3$ film obtained from fitting the $\boldsymbol{E} \parallel [001]$ polarized IR reflectance of the $SrTiO_3/NdGaO_3$ system. Static permittivity obtained from the fit as a function of temperature is shown in the inset.

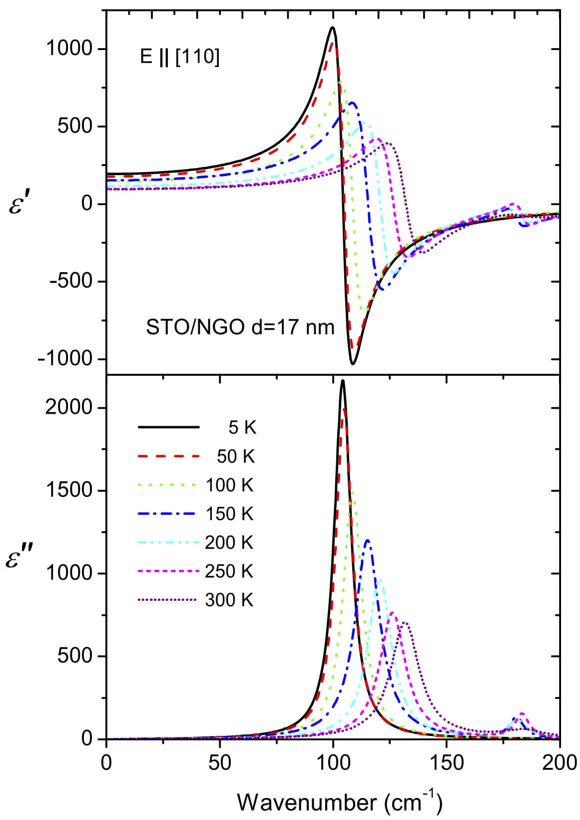

Figure 8. Complex dielectric function of the $SrTiO_3$ film obtained from fitting the $\boldsymbol{E} \parallel [110]$ polarized IR reflectance of the $SrTiO_3/NdGaO_3$ system.

temperature dependence. Softening of the lowest-frequency modes in figures 7 and 8 is clearly seen. The stiffened in-plane TO1 soft mode doublet and its fitted frequencies are shown in figure 9 and compared with the unresolved TO1 doublet from unpolarized measurements in [14].

In figure 10 we compare the temperature dependence of TO phonon frequencies obtained for our $SrTiO_3$ film with those from previous publications on the in-plane compressed $SrTiO_3$ films [14, 17] and on bulk ceramics [40]. Except for at very low temperatures, the phonon frequencies in the ceramics do not differ appreciably from the single-crystal data (see the comparison in [41]). One can see the appreciable TO phonon stiffening in the films, which is most pronounced in the case of the soft TO1 mode. It would be of interest to compare these phonon frequencies with the first-principles phonon calculations of in-plane strained $SrTiO_3$ performed for bulk $SrTiO_3$ crystal [10], but explicit numbers for all the modes were not published, only those for the unstable TO1 mode in the direction of the ferroelectric instability [10]. In this experiment it is the (001) TO1 mode, polarized out-of-plane, that we cannot see due to our near-normal beam incidence. Because of this we cannot determine the in-plane–out-of-plane phonon anisotropy and the in-plane–out-of-plane dielectric anisotropy, which should be quite pronounced, particularly close to the ferroelectric instability. In principle, far IR ellipsometry could be of use. But so far, except for the first attempt to use this technique with a thick $SrTiO_3$ film that neglected this anisotropy [27], no data are available.

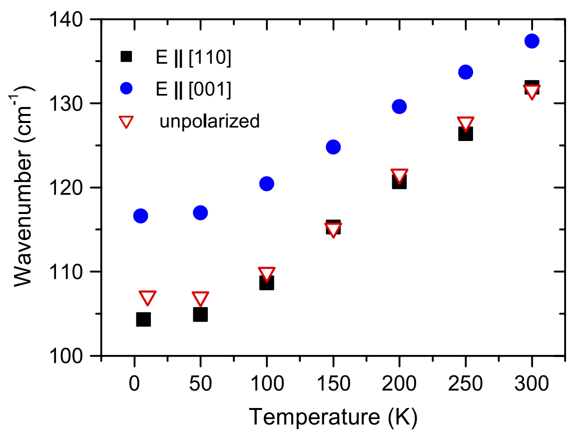

Figure 9. Temperature dependences of the in-plane TO1 mode doublet of the 17 nm $SrTiO_3$ film on the $NdGaO_3$ substrate from the polarized reflectance spectra in comparison with the TO1 mode from the unpolarized IR reflectance spectra of the 50 nm $SrTiO_3$ film on the same substrate [14].

The apparent absence of any sharp ferroelectric transition from both IR and XRD data shows that the film is strongly influenced by the in-plane anisotropy of the $NdGaO_3$ substrate, which produces a biaxial dielectric and phonon anisotropy in the film. Even slightly less compressed ($\sim$0.9%) $SrTiO_3$/LSAT

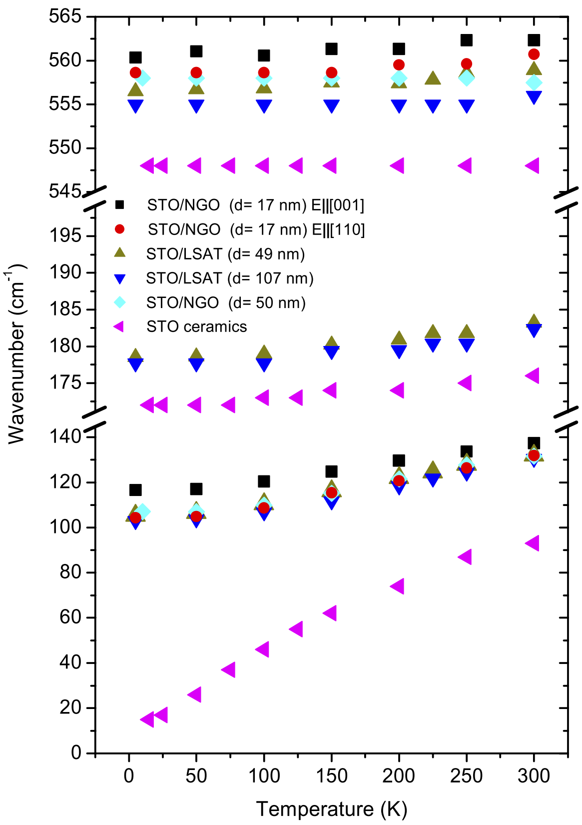

Figure 10. Temperature dependences of the polar modes from the polarized IR reflectance spectra of our $SrTiO_3/NdGaO_3$ film in comparison with other compressively strained $SrTiO_3$ films [14, 17] and bulk ceramics [40].

films with the nearly in-plane isotropic LSAT substrate do not, however, indicate any ferroelectric transition from our IR data [17]. From the present studies, the suggested ferroelectric transition near 150 K on the basis of the previous IR studies of $SrTiO_3/NdGaO_3$ film in unpolarized light, showing the appearance of the very weak silent TO3 mode [14], appears to be an artifact of evaluation that neglected the strong substrate anisotropy. Also the strongly stiffened TO2 phonon frequency [14] is a similar artifact, and the reliable evaluation of the weak TO2 mode parameters is not possible due to strong phonon dispersion in the substrate reflectivity in this frequency range. Summarizing, there is neither IR nor XRD evidence for the out-of-plane ferroelectric phase transition in the compressed $SrTiO_3$ films and further studies are needed.

4. Conclusions

In this study polarized IR reflectance spectroscopy was used to study the in-plane phonon response of a very thin (∼17 nm) epitaxial compressed $SrTiO_3$ film deposited by MBE on an orthorhombic (110) $NdGaO_3$ substrate. The strong in-plane IR anisotropy observed for the bare $NdGaO_3$ substrate was fully explained by the corresponding phonon and electron excitations of B_{1u} and mixed ($B_{2u} + B_{3u}$) symmetries determined from 300 to 5 K. By using these data we were able to study the temperature dependences of the in-plane TO1 and TO4 modes of the $SrTiO_3$ film and reveal their in-plane anisotropy. Appreciable stiffening of all the observed phonons compared to the strain-free bulk samples was found. No indication of any theoretically expected out-of-plane ferroelectric phase transition was found, in accordance with the recent findings [16] from second-harmonic generation and remnant polarization measurements, which show only a very smeared relaxor-like ferroelectric transition below ∼150 K.

Acknowledgments

Financial support by the Czech Science Foundation (Projects Nos 202/09/0682, P204/10/0616, and AVOZ10100520) is gratefully acknowledged. The work was also partially supported by the research programs MSM0021620834, SVV-2010-261307, funding from the EU project NAMASTE, and by the National Science Foundation through Grant No. DMR-0820404. We thank Z Matěj and V Holý for the technical assistance during the XRD experiment and V Nekvasil for enlightening discussions concerning the 4f Nd electronic excitations.

References

[1] Shaw T M, Trolier-McKinstry S and McIntyre P C 2000 *Annu. Rev. Mater. Sci.* **30** 263
[2] Dawber M, Rabe K M and Scott J F 2005 *Rev. Mod. Phys.* **77** 1083
[3] Setter N *et al* 2006 *J. Appl. Phys.* **100** 051606
[4] Schlom D G, Chen L-Q, Eom Ch-B, Rabe K M, Streiffer S K and Triscone J-M 2007 *Annu. Rev. Mater. Res.* **37** 589
[5] Rabe K M, Ahn C H and Triscone J-M (ed) 2007 *Physics of Ferroelectrics: A Modern Perspective* (*Springer Topics in Applied Physics* vol 105) (Berlin: Springer)
[6] Tagantsev A K, Cross L C and Fousek J 2010 *Domains in Ferroic Crystals and Thin Films* (Berlin: Springer)
[7] Haeni J H *et al* 2004 *Nature* **430** 758
[8] Biegalski M D *et al* 2009 *Phys. Rev.* B **79** 224117
[9] Nuzhnyy D, Petzelt J, Kamba S, Kuzel P, Kadlec C, Bovtun V, Kempa M, Schubert J, Brooks C M and Schlom D G 2009 *Appl. Phys. Lett.* **95** 232902
[10] Antons A, Neaton J B, Rabe K M and Vanderbilt D 2005 *Phys. Rev.* B **71** 024102
[11] Li Y L *et al* 2006 *Phys. Rev.* B **73** 184112
[12] Lin C-H, Huang C-M and Guo G Y 2006 *J. Appl. Phys.* **100** 084104
[13] Shirokov V B, Yuzyuk Yu I, Dkhil B and Lemanov V V 2009 *Phys. Rev.* B **79** 144118
[14] Yamada T *et al* 2006 *Phys. Rev. Lett.* **96** 157602
[15] Denev S *et al* 2008 *Phys. Rev. Lett.* **100** 257601
[16] Jang H W *et al* 2010 *Phys. Rev. Lett.* **104** 197601
[17] Nuzhnyy D, Petzelt J, Kamba S, Yamada T, Tyunina M, Tagantsev A K, Levoska J and Setter N 2009 *J. Electroceram.* **22** 297
[18] Hollmann E, Schubert J, Kutzner R and Wordenweber R 2009 *J. Appl. Phys.* **105** 114104
[19] Warusawithana M P *et al* 2009 *Science* **324** 367
[20] Kim Y S, Kim D J, Kim T H, Noh T W, Choi J S, Park B H and Yoon J-G 2007 *Appl. Phys. Lett.* **91** 042908
[21] Kim Y S, Kim J, Moon S J, Choi W S, Chang Y J, Yoon J-G, Yu J, Chung J-S and Noh T W 2009 *Appl. Phys. Lett.* **94** 202906
[22] Tyunina M, Narkilahti J, Plekh M, Oja R, Nieminen R M, Dejneka A and Trepakov V 2010 *Phys. Rev. Lett.* **104** 227601
[23] Calvani P, Capizzi M, Donato F, Dore P, Lupi S, Maselli P and Varsamis C P 1991 *Physica* C **181** 289

[24] Zhang Z M, Choi B I, Flik M I and Anderson A C 1994 *J. Opt. Soc. Am.* B **11** 2252
[25] Ludwig C, Kuhl J and White J O 1997 *Opt. Commun.* **134** 95
[26] Fedorov I, Zelezny V, Petzelt J, Trepakov V, Jelinek M, Trtik V, Cernansky M and Studnicka V 1998 *Ferroelectrics* **208/209** 413
[27] Sirenko A A, Bernhard C, Golnik A, Clark A M, Hao J, Si W and Xi X X 2000 *Nature* **404** 373
[28] Ostapchuk T *et al* 2002 *Phys. Rev.* B **66** 235406
[29] Misra M, Kotani K, Kawayama I, Murakami H and Tonouchi M 2005 *Appl. Phys. Lett.* **87** 182909
[30] Kuzel P, Kadlec F, Nemec H, Ott R, Hollmann E and Klein N 2006 *Appl. Phys. Lett.* **88** 102901
[31] Katayama I, Shimosato H, Rana D S, Kawayama I, Tonouchi M and Ashida M 2008 *Appl. Phys. Lett.* **93** 13903
[32] Brooks C M, Fitting Kourkoutis L, Heeg T, Schubert J, Muller D A and Schlom D 2009 *Appl. Phys. Lett.* **94** 162905
[33] Gervais F 1983 *Infrared and Millimeter Waves* vol 8, ed K J Button (New York: Academic) chapter 7, p 279
[34] Rani N, Gohel V B, Gupta H C, Singh M K and Tiwari L M 2001 *J. Phys. Chem. Solids* **62** 1003
[35] Ubizskii S B, Vasylechko L O, Savytskii D I, Matkovskii A O and Syvorotka I M 1994 *Supercond. Sci. Technol.* **7** 766
[36] Vasylechko L, Akselrud L, Morgeroth W, Bismayer U, Matkovskii A and Savytskii D 2000 *J. Alloys Compounds* **297** 46
[37] Savytskii D I, Ubizskii S B, Matkovskii A O, Suchotski A, Bismayer U, Pashkov V M, Borisov V N, Alexandrovskii A N and Soldatov A V 1999 *Phase Transit.* **70** 57
[38] Kamishima O, Koyama H, Takahashi R, Abe Y, Sato T and Hattori T 2002 *J. Phys.: Condens. Matter* **14** 3905
[39] Savytskii D, Vasylechko L, Senshyn A, Matkovskii A, Bahtz C, Sanjuan M L, Bismayer U and Berkowski M 2003 *Phys. Rev.* B **68** 024101
[40] Petzelt J *et al* 2001 *Phys. Rev.* B **64** 184111
[41] Petzelt J, Ostapchuk T, Gregora I, Kuzel P, Liu J and Shen Z 2007 *J. Phys.: Condens. Matter* **19** 19622